Published in final edited form as:
Nat Med. ; 17(7): 893–898. doi:10.1038/nm.2394.

Simultaneous two-photon imaging of oxygen and blood flow in deep cerebral vessels

Jérôme Lecoq[1,2,3,5,6], **Alexandre Parpaleix**[1,2,3,6], **Emmanuel Roussakis**[4,6], **Mathieu Ducros**[1,2,3], **Yannick Goulam Houssen**[1,2,3], **Sergei A Vinogradov**[4], and **Serge Charpak**[1,2,3]

[1]Institut National de la Santé et de la Recherche Médicale (INSERM), U603, Paris, France

[2]Centre National de la Recherche Scientifique (CNRS), UMR 8154, Paris, France

[3]Laboratory of Neurophysiology and New Microscopies, Université Paris Descartes, Paris, France

[4]Department of Biochemistry and Biophysics, University of Pennsylvania, Philadelphia, Pennsylvania, USA

Abstract

Uncovering principles that regulate energy metabolism in the brain requires mapping of partial pressure of oxygen (PO_2) and blood flow with high spatial and temporal resolution. Using two-photon phosphorescence lifetime microscopy (2PLM) and the oxygen probe PtP-C343, we show that PO_2 can be accurately measured in the brain at depths up to 300 μm with micron-scale resolution. In addition, 2PLM allowed simultaneous measurements of blood flow and of PO_2 in capillaries with less than one-second temporal resolution. Using this approach, we detected erythrocyte-associated transients (EATs) in oxygen in the rat olfactory bulb and showed the existence of diffusion-based arterio-venous shunts. Sensory stimulation evoked functional hyperemia, accompanied by an increase in PO_2 in capillaries and by a biphasic PO_2 response in the neuropil, consisting of an 'initial dip' and a rebound. 2PLM of PO_2 opens new avenues for studies of brain metabolism and blood flow regulation.

Understanding the brain metabolism at rest and during periods of activity requires quantifying the amounts of oxygen entering and exiting selected volumes of neuronal tissue[1]. Previous measurements of PO_2 in the brain have relied mainly on Clark-type oxygen electrodes[2,3]. However, electrodes are invasive and only allow discrete measurements along the insertion path and in the tissue, but not in vessels. One alternative approach is based on oxygen-dependent quenching of phosphorescence[4]. In this method, molecular phosphorescent probes[5] are introduced directly into the blood or interstitial fluid, and external excitation and detection are used to noninvasively retrieve the signal.

Correspondence should be addressed to S.C. (serge.charpak@parisdescartes.fr) or S.A.V. (vinograd@mail.med.upenn.edu).
[5]Current address: James H. Clark Center for Biomedical Engineering and Sciences, Stanford University, Stanford, California, USA.
[6]These authors contributed equally to this work.

Supplementary information is available on the Nature Medicine website.

AUTHOR CONTRIBUTIONS

E.R. and S.A.V. designed and synthesized the oxygen probe. J.L. and M.D. designed and built the optical setup. J.L. and M.D. wrote the LabVIEW program controlling the system and analyzing the data. J.L., A.P., Y.G.H. and S.C. conducted the experiments and analyzed the data. J.L. and S.C. initiated the project. All authors edited the paper.

COMPETING FINANCIAL INTERESTS

The authors declare no competing financial interests.

Here we made use of the recently designed phosphorescent probe PtP-C343[6,7], which allows combining the phosphorescence quenching with two-photon microscopy. A major benefit of two-photon excitation is the confinement of the triplet state, which gives rise to phosphorescence, to the immediate vicinity of the laser focus, thereby eliminating oxygen consumption[8] and formation of reactive oxygen species along the excitation path. The PtP-C343 signal, phosphorescence lifetime τ, is independent of the probe concentration, the pH and the presence of biological macromolecules and is selective for oxygen. PtP-C343 also emits fluorescence, which can be used for fast mapping of the probe distribution in the tissue.

Using 2PLM and PtP-C343, we present depth-resolved micron-scale simultaneous measurements of PO_2 and blood flow in the rodent olfactory bulb. Furthermore, we show that 2PLM allows observation of erythrocyte-associated transients (EATs). Mapping oxygen in various vascular compartments unravels that arterioles contribute to the oxygen content of the neuropil. Measurements of capillary and tissue PO_2 reveal that, at the site of synaptic transmission, odor triggers an increase of vascular PO_2, which is preceded by a dip in tissue PO_2.

RESULTS

2PLM and PtP-C343 sensitivity to oxygen: control experiments

The phosphorescence lifetime of PtP-C343 changes in the range of ~20–40 μs throughout the range of physiological PO_2s7. We used an acousto-optic modulator (AOM)[9] to gate the output of a high repetition rate Ti:sapphire oscillator, creating trains of excitation pulses. These trains (gates) were followed by long off periods (~245 μs) for acquisition of phosphorescence (Fig. 1a,b).

We injected PtP-C343 intravenously into an anesthetized rat (final concentration in the blood ~10 μM) and focused the laser in the lumen of an olfactory bulb capillary ~98 μm below the brain surface (Fig. 1c, top). We set the AOM excitation gate as 2.5 μs and the laser power at 0.7 mW (accounting for 1% duty cycle) (Fig. 1b). We collected the emitted and scattered photons during and after the excitation gate using a photomultiplier tube, whose output was directed into an analog-to-digital converter operating at 1.25 MHz (Fig. 1c, bottom). Plotting the variance at each time point relative to the mean value confirmed that the detection was shot noise limited (Supplementary Fig. 1a). Each decay was fitted with a single-exponential function (Fig. 1d) to extract the phosphorescence lifetime, which was converted into PO_2 using a Stern-Volmer-type calibration plot (Supplementary Fig. 1c).

To establish that the probe's signal is responsive to PO_2 changes *in vivo*, we used two protocols. First, we induced respiratory arrest by injecting a large amount of air through a femoral vein catheter (~0.2–0.4 ml), which led to acute pulmonary embolism. The respiratory arrest was followed by a marked decrease in PO_2 in the olfactory bulb arterioles (Fig. 1e), as was reflected by the phosphorescence signal (control = 78.2 ± 12.4 mm Hg, 3 min after respiratory arrest = 10.8 ± 3.7 mm Hg, n = 4 rats). In the second protocol, we briefly changed the oxygen content in the inhaled air from 21% to 100% and then from 21% to 10% (Fig. 1f). As expected, the arteriolar PO_2 was markedly and reproducibly altered (21% oxygen = 87.8 ± 11.5 mm Hg, 100% oxygen = 146.8 ± 8.2 mm Hg, recovery 21% = 91 ± 6.0 mm Hg, 10% oxygen = 41.1 ± 5.2 mm Hg, recovery 21% = 88.0 ± 12.1 mm Hg). We established that this effect correlated with systemic PO_2 changes, as measured by a pulse oximeter (Supplementary Fig. 1d). These measurements confirmed that the phosphorescence of PtP-C343 provides a functional physiological PO_2-sensitive signal.

Spatial and temporal resolution of oxygen measurements

Previous studies have shown that the triplet state of PtP-C343 in the near-focal volume can be easily saturated by applying multiple high repetition rate pulses[7,10]. Saturation leads to an increase in the emitting volume and subsequent loss of resolution. To attain the highest resolution, excitation must be carried out in the quadratic regime; however, that requires long acquisition times[10]. Therefore, a compromise between spatial and temporal resolution may be chosen.

To establish the optimal excitation regime, we obtained *in vivo* power dependencies of the phosphorescence emission under two-photon excitation. With the excitation gate set at 2.5 μs and the beam focused on a capillary ~98 μm under the surface, quadratic dependence was ensured at moderate laser powers (the region indicated by a black arrow in Fig. 2a, left).

As expected, the precision of the lifetime measurement was dependent on the number of averaged excitation gates (Fig. 2b). For example, 12,000 averages (3 s of acquisition) were sufficient to obtain accurate lifetime values under our measurement conditions. Increasing the probe concentration, the laser power or both permitted faster acquisition without loss of accuracy. We assessed lateral (*xy*) resolution by moving the excitation volume across a capillary (4.1 μm in diameter) (Fig. 2c, left). The weak signal at the capillary boundary, as compared to the strong signal from inside the capillary, confirmed that the oxygen measurement was performed with lateral resolution <1 μm (for point spread function, see Supplementary Fig. 1b).

In many cases, the true diffraction-limited resolution is not required, whereas faster measurement is desirable. We reasoned that by using longer excitation gates, we could attain higher temporal resolution while keeping the excitation volume still sufficiently small[10]. Subsequently, we increased the duration of the excitation gate up to 25 μs (10% duty laser cycle) and simultaneously increased the probe concentration up to ~50 μM. Under the conditions of such long excitation gates, the phosphorescence was outside the quadratic regime (Fig. 2a, right). Nevertheless, at moderate laser powers (0.15–5.0 mW, accounting for 10% duty cycle; depth 80–200 μm), the lateral resolution remained adequate (Fig. 2c, right), whereas lifetime measurements were performed with higher precision (Fig. 2b, right). These experiments confirmed that the probe was confined to the intravascular space.

The depth limit in two-photon imaging depends on both the imaging system and the sample properties[11]. In the rat olfactory bulb with PtP-C343 in the blood (50 μM), we could detect phosphorescence down to the depth of 600 μm using 10% excitation duty cycle (Supplementary Fig. 2a). However, the neighboring neuropil, which was devoid of the probe, also appeared to generate substantial phosphorescence, whose intensity was increasing with depth (Supplementary Fig. 2a). This artifactual result suggested that the near-surface excitation[12] of PtP-C343 in the superficial vessels can limit the accuracy of PO_2 measurements at greater depths. To estimate the contribution of the surface signal to the overall phosphorescence, we measured the ratio of the signal from the vascular compartment (containing the probe) to that of the neuropil (without the probe) at various depths (Supplementary Fig. 2b). We determined that the surface phosphorescence constitutes no more than 10% of the overall signal down to 300 μm. Therefore, we performed our studies at depths not exceeding 300 μm. This depth is sufficient to measure PO_2 in all layers of the rodent olfactory bulb (Supplementary Fig. 3).

PO_2, blood flow and erythrocyte-associated transients

A necessary complementary measurement to local PO_2 is local blood flow, which is usually performed by scanning the beam along the capillary longitudinal axis[13]. However, such scanning is incompatible with single-point PO_2 measurements by 2PLM. In our system, we

detected transient changes, 'shadows', in the signal during the on phase of the AOM (Fig. 3a) while acquiring successive excitation gates. As both the probe and fluorescein-dextran, which was added to the blood to enhance contrast, were dissolved in the blood plasma, we hypothesized that these shadows were caused by red blood cells (RBCs), which outnumber white blood cells by several fold, passing through the excitation volume. Monitoring the amplitude of the signal during the on phase of the cycle (Fig. 3b) allowed extraction of the absolute flow rate of RBCs and provided the local measurement of hematocrit simultaneously with the PO_2 measurement (Fig. 3c). Comparison of the obtained flow rates with those measured with the line-scan method[13,14] confirmed that our pulse-shading technique provides an accurate measurement of the capillary RBC flow (Fig. 3d).

Modeling studies suggest that blood is heterogeneously oxygenated[15]; that is, the regions surrounding RBCs have higher oxygen content than the rest of the plasma. This effect is known as erythrocyte-associated transients (EATs), and its existence has been demonstrated experimentally in the peripheral vascular system[16,17]. However, these results are continuously debated, as previous measurement techniques were incapable of micron-scale resolution[18].

At its typical velocity (~1 mm s^{-1}), an RBC passes by the 2PLM excitation volume in less than 10 ms, which is too fast to measure PO_2 values at different distances from the RBC to detect the EAT effect. Fortunately, shadows produced by RBCs (Fig. 3a,b) provided excellent reference points for averaging phosphorescence decays corresponding to various distances from the RBCs' boundaries (Fig. 3e). In a typical experiment, we focused the laser on a capillary and detected all passing RBCs by their shadows during the AOM-on phase. We then grouped the phosphorescence decays on the basis of their distance from the RBC boundaries and averaged and analyzed them to give the corresponding PO_2 values. We made these measurements at the highest resolution (quadratic regime), as we expected the EATs to be restricted to the immediate vicinity of RBCs.

Indeed, we found the phosphorescence lifetimes to be shorter near the RBCs (Fig. 3f). We repeated measurements in eleven capillaries, and the data unambiguously confirmed considerably higher PO_2 values in the immediate vicinity of RBCs (Fig. 3g) (PO_2 = 57.9 ± 8.5 mm Hg) than in the bulk plasma (PO_2 = 31.2 ± 3.2 mm Hg; $P = 0.0006$, $n = 11$, paired t test), making up for 26.6 ± 5.4 mm Hg ($n = 11$) gradient in PO_2. The latter value is in the same range, although slightly higher than reported for the peripheral vasculature[16,17]. In five capillaries we consecutively measured RBC flow rates by performing line scans to correct for the variations in the RBCs speed and plotted PO_2 versus the distance from the RBC wall (Fig. 3h). We observed the EATs in the first 5 μm from the RBC boundary.

Diffusional shunt of oxygen between arterioles and venules

Modeling studies of oxygen diffusion usually assume certain vascular geometries to compute oxygen levels in the neuronal tissue[19]. The relative contributions of arterioles, capillaries and venules to the oxygen supply in the brain are still under debate because experimental PO_2 measurements in various tissue compartments are difficult to perform[20]. The high rate of the metabolism of neuronal tissue should enhance the vessel-to-tissue gradient and favor oxygen diffusion from arterioles. The olfactory bulb nerve layer is unique in its very low content of capillaries[2,13]. We reasoned that if arterioles act as a substantial diffusive supply of oxygen to the neuropil, diffusional shunts between arterioles and venules, bypassing capillaries[21,22], would be detectable by measuring PO_2 in venules running close to or crossing arterioles in the nerve layer.

We were able to identify a venule by its low oxygen content before crossing an arteriole (Fig. 4a). PO_2 in the venule increased from 48 mm Hg (distance between venule and

arteriole = 38 μm) to 57 mm Hg (distance = 27 μm). To eliminate the possibility that the PO_2 values followed random vascular fluctuations, we repeated the measurement (in quadratic regime) in the forward and reverse order (2.5 s per point) along the venule axis (Fig. 4b). The increase was observed in all the tested rats (Fig. 4c). Measurements in nine crossings showed that the PO_2 in the venule increased on average by ~9 mm Hg upon crossing an arteriole (Fig. 4d). Thus, we conclude that such diffusional shunts may occur at each crossing throughout the central nervous system (CNS), making arterioles key players in the oxygen supply to the neuropil.

Dynamics of PO_2 in capillaries and neuropil during odor

Could 2PLM be used to monitor changes in vascular and tissue PO_2 during neuronal activation? We have previously shown that in olfactory bulb glomeruli, odor stimulation triggers local functional hyperemia that follows postsynaptic neuronal activation after 1–2 s[13,23]. Using the same model[24], we labeled olfactory receptor neuron terminals with Calcium Green-1 dextran, a low-affinity calcium (Ca^{2+}) probe, and capillaries with fluorescein-dextran (see Online Methods). Inhalation of an odorant triggered a presynaptic Ca^{2+} increase followed by a local increase in the RBC flow (Fig. 5a), which we detected by the classical line-scan method. In the second step, we injected PtP-C343 (~50 μM) and measured PO_2 with high temporal resolution (25 μs excitation gate, 10% duty cycle) (Fig. 2). Notably, at 50 μM concentration, PtP-C343 did not affect odor-evoked Ca^{2+} responses, suggesting that the probe is neither toxic nor phototoxic at this meaurement regime. Further, we performed measurements of PO_2 and RBC flow (Fig. 5b) during odor stimulation in the same capillary (151 μm deep). We analyzed only those decays that were further away from the RBCs, thus limiting the PO_2 measurements to the bulk plasma. This analysis (Fig. 5b–d) revealed large and reproducible increases in the PO_2 accompanying the local functional hyperemia.

Finally, we investigated whether 2PLM could be used to detect changes in tissue PO_2 in the glomerular neuropil during odor stimulation[2]. We inserted a glass pipette containing PtP-C343 (1 mM solution) into an odor-responsive glomerulus, in which presynaptic Ca^{2+} signals could be detected in olfactory neuron terminals upon odorant inhalation. We applied pressure to the pipette until PtP-C343 fluorescence could be detected in a part of the glomerular volume (Fig. 5e). We performed point measurements of PO_2 at a distance from the pipette tip (>10 μm), showing that the odor stimulation induced reproducible biphasic PO_2 changes (Fig. 5e) consisting of the initial dip, followed by a rebound, characteristic of an immediate oxygen consumption, followed by an increase resulting from the local functional hyperemia (Fig. 5e)[2]. The dip was observed in the neuropil of each of the five rats tested (total of 29 odor applications).

DISCUSSION

Our results demonstrate that 2PLM is an efficient tool for mapping oxygen levels in both microvascular and extravascular compartments with high spatial and temporal resolution. One major concern related to the use of molecular probes is their phototoxicity. Our conclusion is that PtP-C343 was neither toxic nor phototoxic over the duration of our experiments. At concentrations of 10 μM–50 μM in the blood, PtP-C343 did not affect odor-evoked Ca^{2+} or vascular responses over a period of 3–5 h. Photoactivation of PtP-C343 did not induce any detectable toxicity, even when the probe was used at 50 μM concentration in combination with 10% excitation duty cycle. Finally, injection of PtP-C343 in the neuropil (1 mM in the pipette) did not seem to have any detectable effect on Ca^{2+} and vascular responses.

Previous attempts to image oxygen have relied on independent techniques to provide blood flow recordings. Here we show that it is possible to simultaneously measure blood flow and PO_2 in individual capillaries. Simultaneous recordings are necessary to assess the effect of both parameters on oxygen diffusion in tissue. Our data confirm that PO_2 and blood flow are highly correlated[25]. Furthermore, by directly observing EATs we confirmed that oxygen is highly modulated between individual RBCs in the CNS vasculature. Modeling studies of oxygen diffusion in the CNS should benefit from these results, which will allow more accurate prediction of oxygen levels in the neuropil.

The importance of arterioles for the oxygen supply has been debated in the literature[20]. Our results show that arterioles provide oxygen to venules at arteriovenule crossings, making oxygen content in the brain strongly dependent on the arterial content. In previous studies, oxygen electrodes had to be placed near or pressed against the vessel walls to measure oxygen gradients in the vasculature, as intraluminal recordings instantaneously generated thromosis[26]. In contrast, 2PLM provides a noninvasive measurement of true intraluminal oxygen gradients[27] along microvascular trees.

Finally, we have shown the possibility of simultaneous measurements of oxygen and blood flow in individual capillaries during functional hyperemia in response to a physiological stimulus. Extending the measurements to the entire vascular compartment will provide key insights into the origin of the functional magnetic resonance imaging blood-oxygen-level dependence signal. Concomitant measurements of PO_2 in vessels and in the surrounding tissue will allow quantification of oxygen exchange between these two compartments during different states of brain activation.

METHODS

Methods and any associated references are available in the online version of the paper at http://www.nature.com/naturemedicine/.

Supplementary Material

Refer to Web version on PubMed Central for supplementary material.

Acknowledgments

We thank V. De Sars and N. Chaari for technical assistance in the design of electronic circuits, G. Bouchery for her help in rat surgery, C. Pouzat for help with statistical analysis and L.E. Sinks for discussion of the phosphorescence microscopy data. Support was provided by INSERM, CNRS, the Région Ile de France (Sesame program), the Fondation Bettancourt Schueller the Leducq Foundation, the Human Frontier Science Program Organization, the European Commission FP6 (LSHM-CT-2007-037765), the Fondation pour la Recherche Médicale and the US National Institutes of Health (grant EB007279). Photophysical characterization of the probe was performed in the Ultrafast Optical Processes Laboratory at the University of Pennsylvania (US National Institutes of Health grant P41-RR001348).

References

1. Raichle ME, Mintun MA. Brain work and brain imaging. Annu Rev Neurosci. 2006; 29:449–476. [PubMed: 16776593]
2. Lecoq J, et al. Odor-evoked oxygen consumption by action potential and synaptic transmission in the olfactory bulb. J Neurosci. 2009; 29:1424–1433. [PubMed: 19193889]
3. Ndubuizu O, LaManna JC. Brain tissue oxygen concentration measurements. Antioxid Redox Signal. 2007; 9:1207–1219. [PubMed: 17536959]

4. Rumsey WL, Vanderkooi JM, Wilson DF. Imaging of phosphorescence: a novel method for measuring oxygen distribution in perfused tissue. Science. 1988; 241:1649–1651. [PubMed: 3420417]
5. Lebedev AY, et al. Dendritic phosphorescent probes for oxygen imaging in biological systems. ACS Appl Mater Interfaces. 2009; 1:1292–1304. [PubMed: 20072726]
6. Finikova OS, et al. Energy and electron transfer in enhanced two-photon-absorbing systems with triplet cores. J Phys Chem A. 2007; 111:6977–6990. [PubMed: 17608457]
7. Finikova OS, et al. Oxygen microscopy by two-photon–excited phosphorescence. ChemPhysChem. 2008; 9:1673–1679. [PubMed: 18663708]
8. Golub AS, Pittman RN. PO_2 measurements in the microcirculation using phosphorescence quenching microscopy at high magnification. Am J Physiol Heart Circ Physiol. 2008; 294:H2905–H2916. [PubMed: 18375716]
9. Estrada AD, Ponticorvo A, Ford TN, Dunn AK. Microvascular oxygen quantification using two-photon microscopy. Opt Lett. 2008; 33:1038–1040. [PubMed: 18483504]
10. Sinks LE, et al. Two-photon microscopy of oxygen: polymersomes as probe carrier vehicles. J Phys Chem B. 2010; 114:14372–14382.
11. Oheim M, Beaurepaire E, Chaigneau E, Mertz J, Charpak S. Two-photon microscopy in brain tissue: parameters influencing the imaging depth. J Neurosci Methods. 2001; 111:29–37. [PubMed: 11574117]
12. Theer P, Denk W. On the fundamental imaging-depth limit in two-photon microscopy. J Opt Soc Am A Opt Image Sci Vis. 2006; 23:3139–3149. [PubMed: 17106469]
13. Chaigneau E, Oheim M, Audinat E, Charpak S. Two-photon imaging of capillary blood flow in olfactory bulb glomeruli. Proc Natl Acad Sci USA. 2003; 100:13081–13086. [PubMed: 14569029]
14. Kleinfeld D, Mitra PP, Helmchen F, Denk W. Fluctuations and stimulus-induced changes in blood flow observed in individual capillaries in layers 2 through 4 of rat neocortex. Proc Natl Acad Sci USA. 1998; 95:15741–15746. [PubMed: 9861040]
15. Hellums JD. The resistance to oxygen transport in the capillaries relative to that in the surrounding tissue. Microvasc Res. 1977; 13:131–136. [PubMed: 859450]
16. Barker MC, Golub AS, Pittman RN. Erythrocyte-associated transients in capillary PO_2: an isovolemic hemodilution study in the rat spinotrapezius muscle. Am J Physiol Heart Circ Physiol. 2007; 292:H2540–H2549. [PubMed: 17277027]
17. Golub AS, Pittman RN. Erythrocyte-associated transients in PO_2 revealed in capillaries of rat mesentery. Am J Physiol Heart Circ Physiol. 2005; 288:H2735–H2743. [PubMed: 15695557]
18. Tsai AG, et al. Effect of oxygen consumption by measuring method on PO_2 transients associated with the passage of erythrocytes in capillaries of rat mesentery. Am J Physiol Heart Circ Physiol. 2005; 289:H1777. [PubMed: 16162870]
19. Tsoukias NM, Goldman D, Vadapalli A, Pittman RN, Popel AS. A computational model of oxygen delivery by hemoglobin-based oxygen carriers in three-dimensional microvascular networks. J Theor Biol. 2007; 248:657–674. [PubMed: 17686494]
20. Tsai AG, Johnson PC, Intaglietta M. Oxygen gradients in the microcirculation. Physiol Rev. 2003; 83:933–963. [PubMed: 12843412]
21. Ellsworth ML, Pittman RN. Arterioles supply oxygen to capillaries by diffusion as well as by convection. Am J Physiol. 1990; 258:H1240–H1243. [PubMed: 2331012]
22. Stein JC, Ellis CG, Ellsworth ML. Relationship between capillary and systemic venous PO_2 during nonhypoxic and hypoxic ventilation. Am J Physiol. 1993; 265:H537–H542. [PubMed: 8368357]
23. Chaigneau E, et al. The relationship between blood flow and neuronal activity in the rodent olfactory bulb. J Neurosci. 2007; 27:6452–6460. [PubMed: 17567806]
24. Shepherd GM, Charpak S. The olfactory glomerulus: a model for neuro-gliovascular biology. Neuron. 2008; 58:827–829. [PubMed: 18579073]
25. Nwaigwe CI, Roche MA, Grinberg O, Dunn JF. Brain tissue and sagittal sinus pO_2 measurements using the lifetimes of oxygen-quenched luminescence of a ruthenium compound. Adv Exp Med Biol. 2003; 530:101–111. [PubMed: 14562708]

26. Vovenko E. Distribution of oxygen tension on the surface of arterioles, capillaries and venules of brain cortex and in tissue in normoxia: an experimental study on rats. Pflugers Arch. 1999; 437:617–623. [PubMed: 10089576]

27. Sakadzić S, et al. Two-photon high-resolution measurement of partial pressure of oxygen in cerebral vasculature and tissue. Nat Methods. 2010; 7:755–759. [PubMed: 20693997]

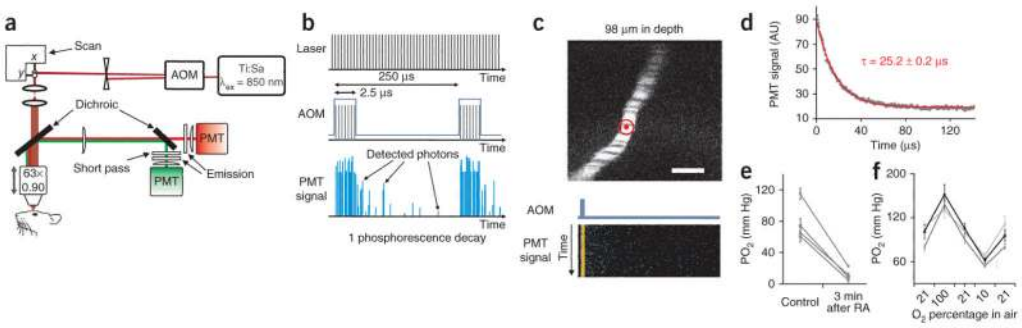

Figure 1.

Measurements of PO_2 in deep cerebral vessels using probe PtP-C343. (**a**) Experimental setup. An AOM is placed in the excitation path of a standard two-photon microscope, enabling fast repetitive on-off switching of the laser excitation. (**b**) The probe is excited by a brief gate (2.5 µs) of femtosecond pulses from a Ti:sapphire laser (λ_{ex} = 850 nm, <250 fs, 76 MHz), followed by a phosphorescence detection period (~250 µs). The fluorescence emitted by PtP-C343 is detected by a photomultiplier tube (PMT) in the green channel (PMT1); the phosphorescence is detected by PMT2 in the red channel. (**c**) Top, intravenous (i.v.) injection of PtP-C343 and fast scanning with detection of fluorescence reveals capillary in the rat olfactory bulb. Phosphorescence is measured at selected spots (red in the capillary lumen). Scale bar, 10 µm. Bottom, successive phosphorescence acquisition cycles displayed as an image. Each horizontal line is one complete cycle, whereas the vertical axis shows successive cycles. (**d**) Phosphorescence decay obtained by averaging of 40,000 excitation gates, fitted to a single exponential (red). (**e**) Respiratory arrest (RA) induced by air injection into the femoral vein. (**f**) Effect of changes in oxygen content in the inhaled air from 21% to 100% or 10% on PO_2. Error bars indicate s.e.m.

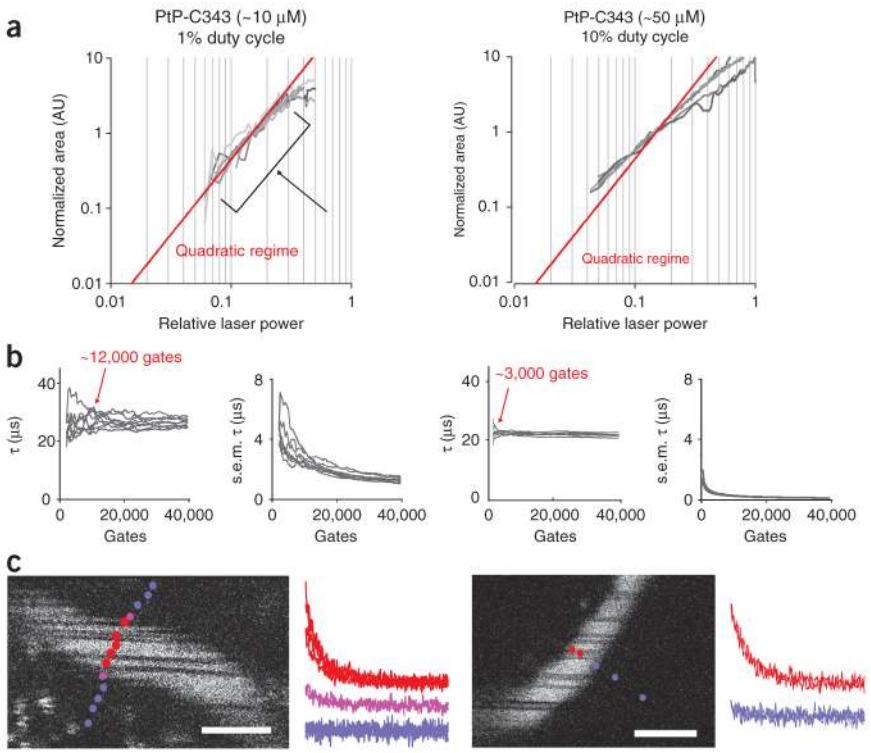

Figure 2.

Temporal and spatial resolution of two-photon phosphorescence measurement. (**a**) Log-log plots of the phosphorescence integrated intensity (area under the decay curve after subtraction of the baseline) versus average excitation power. Left, AOM gate 2.5 μs. Maximal power shown: 275 mW after the objective, or 2.7 mW, taking into account 1% duty cycle; focal spot depth 80 μm. Red line (slope = 2) corresponds to pure quadratic dependence. The black arrow indicates the region of quadratic dependence (up to 50–60 mW). Right, AOM gate 25 μs (average laser power ~0.5–0.6 mW, 10% duty cycle). The phosphorescence emission is outside the quadratic regime throughout the entire power range. AU, arbitrary units. (**b**) Precision of the lifetime (τ) measurement as a function of the number of averages, their duration and PtP-C343 concentration (injected i.v.). Left, AOM gate: 2.5 μs (PtP-C343 concentration: ~10 μM, average laser power ~0.5–0.6 mW). Lifetime measurements were performed in eight capillaries at ~100 μm depth. 12,000 averages (~3 s) are sufficient to reach the desired precision. Right, AOM gate 25 μs (PtP-C343 concentration ~50 μM, average laser power ~7 mW). 3,000 gates (~0.80 s) are sufficient to achieve the same precision as in left. (**c**) Spatial confinement of phosphorescence measurements under different excitation regimes (left, AOM gate 2.5 μs; right, AOM gate 25 μs). Point measurements were performed perpendicularly to the longitudinal axis of two capillaries. Phosphorescence decays were observed in the capillary lumen (red dots) but not in the neuropil (blue dots). Measurements at capillary boundaries produced weak signal (purple dots). Scale bars, 5 μm.

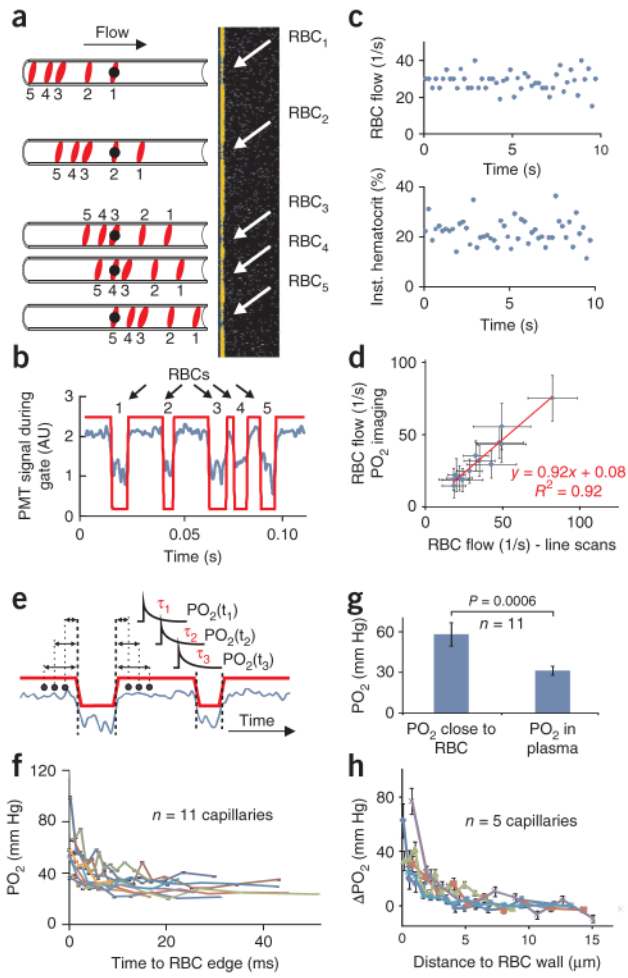

Figure 3.

Simultaneous measurements of RBC flow and PO_2 using fluorescence and phosphorescence of PtP-C343. (**a**) RBC detection. The fluorescence of PtP-C343 in the plasma during the excitation gate is shadowed by passing RBCs (white arrows on right pictures corresponding to individual schematics on the left). (**b**,**c**) Automatic detection of RBC transients (**b**) allows extraction of local RBC flow rates (**c**, top) as well as the estimation of instantaneous hematocrit (**c**, bottom). (**d**) Consecutive measurements of RBC flow using the line-scan approach and our pulse-shading method (n = 13 vessels). (**e**–**h**) Erythrocyte-associated transients (EATs) in single capillaries. (**e**) Two RBC fluorescence transients are used as time markers to determine locations of the phosphorescence measurements relative to each RBC. (**f**) Change in the PO_2 near a single RBC. Decays were acquired during 200 s (20 recordings, 10 s each) in eleven capillaries. Each decay is an average of 40,000 gates. (**g**) PO_2 values measured in the plasma and in the close vicinity of RBCs. (**h**) Consecutive line scans acquired in five capillaries to measure the corresponding distance. Error bars represent s.e.m.

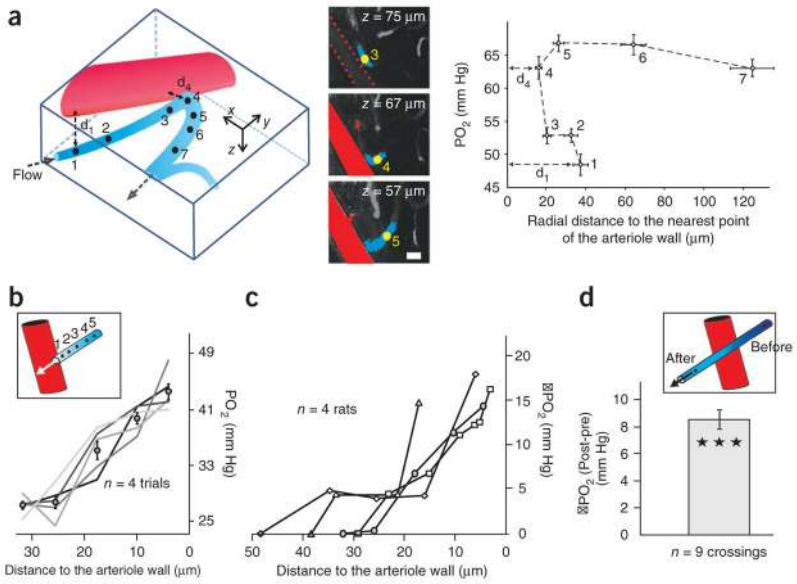

Figure 4.

Diffusional shunt of oxygen between arterial and venous compartments in the olfactory nerve layer. (**a**) PO_2 measurements along a venule approaching an arteriole. Left, three-dimensional reconstruction of the two vessels (extracted from a two-photon fluorescence stack of images). Venule is in blue and arteriole in red. Right, seven successive PO_2 measurements (three to six acquisitions at each point) in the venule. Scale bars, 40 µm. (**b**) Diffusional shunt of oxygen is independent of vascular fluctuations. The venule lies in the *xy* plane. Measurements of PO_2 were performed repetitively in five points (2.5 s per point). (**c**) Venous PO_2 as a function of the distance, measured in four animals. (**d**) Diffusional shunt of oxygen at complete arteriolar-venular crossings. Error bars represent s.e.m.

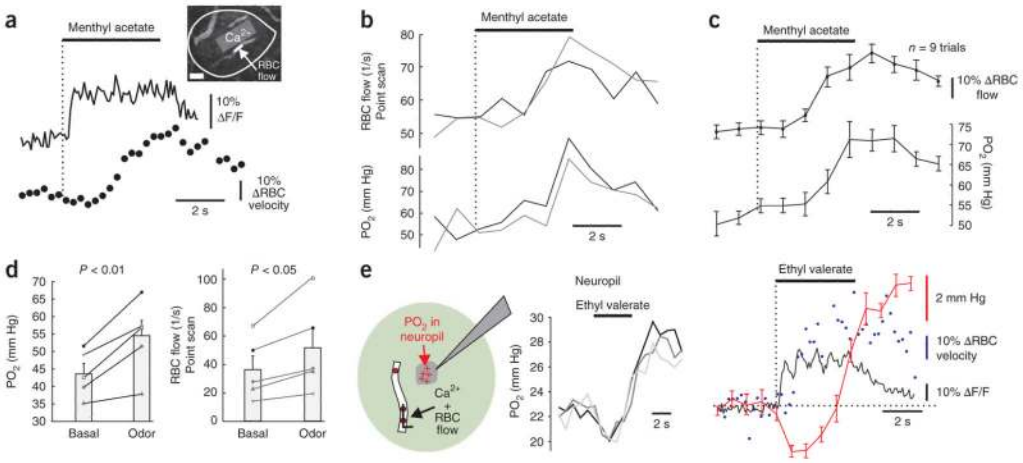

Figure 5.

Functional hyperemia, vascular and neuropil PO_2 dynamics in response to odor stimulation. (**a**) Neuronal and vascular responses during odor stimulation. Inset, glomerulus with boundaries that were outlined by olfactory receptor neuron terminals labeled with Calcium Green-1 dextran, and capillaries labeled with fluorescein-dextran. The presynaptic Ca^{2+} response was recorded over the rectangle. RBC velocity was obtained from line scans drawn in the capillary segment, indicated by the arrow. Scale bar, 20 μm. (**b**) RBC and PO_2 responses in the same capillary. I.v. injection of PtP-C343 allows detection of the concomitant increases in the RBC flow and PO_2 (point measurements of PtP-C343 fluorescence and phosphorescence, respectively) in response to the odorant inhalation (two trials). (**c**) Mean RBC flow and PO_2 responses (nine trials). (**d**) Summary of vascular responses in five rats. (**e**) PO_2 dynamics in the glomerular neuropil. Left, schematic of the experiment. Middle, three successive measurements of PO_2 in neuropil in response to odor stimulation. Right, superposition of presynaptic Ca^{2+}, RBC and PO_2 responses in the same glomerulus. Error bars indicate s.e.m.